Environ. Sci. Technol. **2005**, *39,* 8948−8957

On the Nonlinear Relationship between k_{obs} and Reductant Mass Loading in Iron Batch Systems

DAVID M. CWIERTNY AND
A. LYNN ROBERTS*

Department of Geography and Environmental Engineering, 313 Ames Hall, Johns Hopkins University, 3400 North Charles Street, Baltimore, Maryland 21218

A first-order relationship between reaction rate and reductant loading is commonly invoked (but rarely verified) for granular iron batch systems. In this study, a linear relationship between the pseudo-first-order rate constant (k_{obs}) for polyhalogenated alkane reduction and iron mass loading (ρ_m) was only obtained when reduction appeared to be mass-transport-limited. For most alkyl polyhalides, a nonlinear relationship was observed under various experimental conditions, causing surface-area-normalized rate constants (k_{SA}) to decrease by as much as an order of magnitude with increasing ρ_m. While a detailed explanation for this nonlinearity remains unclear, the reaction order in ρ_m (from plots of log(k_{obs}) versus log(ρ_m)) approached unity as the system pH decreased, suggesting that the behavior may be linked to changes in the thickness of a passive oxide overlayer. We obtained strong linear correlations between k_{obs} values and the concentration of aqueous iron(II) generated over a 24 h period in batch systems with that same ρ_m. Equally strong correlations were obtained when k_{obs} was related to the summed concentration of protons and water reduced over an equivalent time interval at that same ρ_m. Such correlations suggest a possible link between those sites responsible for proton/water reduction and the surface species participating in alkyl polyhalide reduction by granular iron.

Introduction

Granular iron permeable reactive barriers (PRBs) represent a promising treatment alternative for groundwater contaminated with halogenated organic solvents such as carbon tetrachloride (CCl_4) (*1*) and trichloroethylene (TCE) (*2*). Despite extensive laboratory and field-scale investigations over the past decade, many fundamental issues surrounding the chemistry of granular iron remain unclear. In particular, a better understanding of the surface sites responsible for organohalide reduction would potentially allow for improved engineering design and hence performance of granular iron PRBs.

A surface-area-normalized kinetic model is commonly applied to organohalide reduction in granular iron batch systems. This model assumes that the rate of reaction between iron and a contaminant *C* is first-order with respect to both total iron surface area and contaminant concentration (*3*). Such an assumption allows the reaction rate to be expressed as follows

$$\frac{-d[C]}{dt} = k_{SA} a_s \rho_m [C] = k_{obs}[C] \quad (1)$$

where k_{SA} (L h^{-1} m^{-2} or m s^{-1}) is a surface-area-normalized rate constant, a_s (m^2 g^{-1}) is the iron specific surface area (typically determined by N_2- or Kr-BET), and ρ_m (g L^{-1}) is the iron mass loading in the system. Values of k_{SA} are determined by normalizing the pseudo-first-order rate constant for contaminant degradation (k_{obs}) by the iron surface area concentration (ρ_a in m^2/L, where ρ_a is the product of a_s and ρ_m) as shown in eq 2.

$$k_{SA} = \frac{k_{obs}}{a_s \rho_m} = \frac{k_{obs}}{\rho_a} \quad (2)$$

This model requires that both the fraction of total iron surface area that is redox-active and the intrinsic reactivity of the iron be essentially constant for all values of ρ_m.

Prior studies provide conflicting results as to the validity of eq 1, as certain investigations (*1*, *4*−*9*) claim a linear relationship between iron reactivity and ρ_m (or ρ_a), while others (*6*, *10*−*15*) report a distinctly nonlinear relationship. In the latter case, iron reactivity (expressed as a reaction rate or as a k_{obs} value) most often increases nearly linearly with ρ_m at low loadings, only to reach an apparent plateau at higher ρ_m. Explanations proffered for this behavior include a shift from mass-transfer-limited kinetics to kinetics limited by rates of chemical reaction (*11*) or inefficient reactor mixing at high ρ_m (*2*). To date, however, the underlying basis of the reported nonlinearity has yet to be adequately explored. Nor have the explanations for such behavior postulated by previous investigators been rigorously tested.

Deviations from a linear relationship are of potentially great importance, as k_{SA} values reported for granular iron batch systems have numerous applications. Most often used for intersystem reactivity comparisons (*3*), k_{SA} values represent the primary means for comparing nanoscale iron reactivity to that of traditional, larger-scale iron particles (*16*−*19*). They have also been used to develop quantitative structure−activity relationships for organohalides that might prove useful for predicting rate constants of uninvestigated compounds in zero valent metal systems (*20*−*22*), while also providing a means of scaling up laboratory experimental results for the design and modeling of field-scale PRBs (*23*).

A nonlinear relationship between k_{obs} and ρ_m would result in k_{SA} values that are not truly constant but rather vary as a function of iron loading. In such a case, k_{SA} values would be of questionable utility in any of the aforementioned applications. A nonlinear relationship may also have theoretical implications, suggesting that the role of the iron surface in organohalide reduction is more complex than currently envisioned. Furthermore, if an explanation for the nonlinear relationship could be elucidated, then valuable insights into the nature of the surface site(s) responsible for organohalide reduction may emerge.

In this study, batch experiments were conducted over a range of iron mass loadings to test whether the relationship between k_{obs} for polyhalogenated ethane reduction and ρ_m is indeed first-order. Alkyl polyhalides investigated include 1,1,1-trichloroethane (1,1,1-TCA), 1,1,2-trichloroethane (1,1,2-TCA), 1,1,2,2-tetrachloroethane (1,1,2,2-TeCA), 1,1,1,2-tetrachloroethane (1,1,1,2-TeCA), pentachloroethane (PCA), hexachloroethane (HCA), 1,1-dibromoethane (1,1-DBA), 1,2-dibromoethane (1,2-DBA), and 1-bromo-2-chloroethane (BCA). Rate constants for mass transport (or $k_L a$ values) were also estimated for these species to examine the possible

* Corresponding author phone: (410)516-4387; fax: (410)516-8996; e-mail: lroberts@jhu.edu.

10.1021/es050472j CCC: $30.25 © 2005 American Chemical Society
Published on Web 10/14/2005

influence of mass-transfer limitations on the relationship between k_{obs} and ρ_m. Additional batch studies emphasized experimental factors, particularly those postulated by prior investigators, that could produce deviations from a linear, first-order relationship. These factors included the apparatus and speed used to mix reactors, initial organohalide concentration, duration of system equilibration prior to organohalide addition to the reactor, buffer composition, and system pH. The greatest effort was devoted to elucidating the influence of system pH, which was nearly constant during the reaction between alkyl polyhalides and iron, but increased substantially over the 24 h period prior to initiation of the reaction. Finally, additional efforts were made to examine system variables other than ρ_m that relate to iron reactivity, and that may provide valuable insights into the nature of surface sites primarily responsible for polyhalogenated ethane reduction.

Experimental Section

Chemicals. The alkyl polyhalides investigated were 1,1,1-TCA (99.5%, Aldrich), 1,1,2-TCA (99%, TCI), 1,1,1,2-TeCA (99%, Aldrich), 1,1,2,2-TeCA (98+%, Aldrich), PCA (95%, Aldrich), HCA (99%, Aldrich), 1,1-DBA (98%, TCI), 1,2-DBA (99+%, Aldrich), and BCA (98%, TCI), while the following species were used in the identification and quantification of reduction products: tetrachloroethylene (99.9%, Aldrich), trichloroethylene (98%, Aldrich), 1,1-dichloroethylene (99%, Aldrich), *cis*-dichloroethylene (97%, Aldrich), *trans*-dichloroethylene (98%, Aldrich), vinyl chloride (2000 μg/mL in methanol, Supelco), 1,1-dichloroethane (99%, TCI America), bromoethane (99%, TCI), and 2-butyne (99%, Aldrich). Gas standards of ethane, ethylene, and *cis*-2-butene (1000 ppm of each in N_2) were acquired from Scott Specialty Gases.

Buffer solutions of either 50 mM Tris (tris(hydroxymethyl)-aminomethane), 50 mM sodium bicarbonate, or 50 mM MES (2-(4-morpholino)ethanesulfonic acid) in 0.1 M NaCl were prepared using deionized water (Milli-Q Plus UV, Millipore) and were deoxygenated by sparging (1 h/L) with either N_2 (Tris and MES) or a CO_2/N_2 mix (bicarbonate). When necessary, solution pH was adjusted with 1 N HCl or NaOH that had been deoxygenated by N_2 sparging. All solutions were stored within an anaerobic chamber (5% H_2/95% N_2 atmosphere) until use.

Metal Preparation. Fisher electrolytic iron (100 mesh) was the metallic reductant used for all experiments. Iron particles were pretreated with 1 N HCl for 10 min as detailed in Fennelly and Roberts (*24*) and were used within 24 h of preparation. The iron's specific surface area was determined to be 0.4 ($\pm$0.1) $m^2\ g^{-1}$ by Kr-BET adsorption measurements of triplicate samples using a Beckman Coulter SA3100 surface area analyzer.

Experimental Systems. Experiments were conducted in serum bottles (160 mL, nominal volume) sealed with Teflon-faced butyl rubber septa (Wheaton). Within an anaerobic chamber, iron powder was weighed into reactors that were then filled with buffer solution. Initial pH values (pH_0) ranged between 6.90 and 8.65 for Tris (pK_a 8.1) and 5.50 and 6.5 for MES (pK_a 6.2), while experiments with carbonate buffer (pK_{a1} 6.3, pK_{a2} 10.3) were conducted at a pH_0 of 7.30 (pH_0 values correspond to the solution pH prior to contact with granular iron). Iron mass loadings ranged from 0.16 to 28.3 g/L, with control studies for each species also being conducted in the absence of granular iron. After assembly, reactors were removed from the chamber and were equilibrated on a mixing device for ~24 h prior to alkyl polyhalide addition to allow for stabilization of system pH. To assess the equilibration period's influence on iron reactivity, experiments were also conducted in which 1,1,1-TCA was added immediately after reactor assembly.

Most alkyl polyhalides were introduced to reactors via a 50 μL spike from a 0.32 M deoxygenated methanolic stock solution (generally resulting in ~0.025% methanol by weight and an initial organohalide concentration of ~100 μM). Because of its low solubility in both methanol and water, HCA required a 400 μL spike from a 0.016 M methanolic stock solution (resulting in ~0.2% methanol by weight and an initial HCA concentration of ~40 μM). Additional experiments investigated the influence of the initial 1,1,1-TCA concentration (ranging from ~5 to ~200 μM) on rates of reduction in systems with 1.6 g/L iron. For these experiments, methanolic spiking solutions with various 1,1,1-TCA concentrations (8−320 mM) were used so that the resulting methanol concentration was constant at 0.05% in all systems. In all cases, the methanol (HPLC grade, J. T. Baker) was deoxygenated via sparging with N_2 prior to use.

Mixing Devices. Three devices were employed in studying 1,1,1-TCA reduction. These were a custom jar mill (U. S. Stoneware), which mixed bottles at 45 rpm about their longitudinal axes, a rotator (Cole-Palmer), which mixed bottles at 45 rpm about their longitudinal axes, and a table shaker (Eberbach), which mixed bottles horizontally at 250 rpm. The jar mill was also used to investigate the influence of mixing rate (20, 45, and 60 rpm) on 1,1,1-TCA reduction.

Determination of Aqueous Fe^{II} Concentrations. The concentration of Fe^{II}(aq) generated in batch systems was quantified using the colorimetric reagent ferrozine (*25*). Within an anaerobic chamber, 1 mL of reactor solution was passed through a 0.22 μm syringe filter (Millipore) and was added to 1 mL of 1 N HCl. An aliquot of this acidified sample (200 μL) was then added to 4 mL of 1 g/L ferrozine in 50 mM HEPES (pH 7). Samples were removed from the chamber and were analyzed on a Shimadzu UV-1601 UV−visible spectrophotometer (λ = 562 nm). Standards of Fe^{II}(aq) were generated from solutions of $FeCl_2{\cdot}4H_2O$ in Tris buffer and were prepared for UV−vis analysis in a manner identical to the experimental samples.

Headspace Evolution and System pH. Although initially free of headspace, significant amounts (as much as 10 mL in certain cases) generally developed over the duration of the experiments, presumably from the reduction of water to H_2 by iron. Headspace evolution was greatest at low pH_0 and/or high ρ_m and was only observed to occur after the reactor was spiked with an alkyl polyhalide, as negligible headspace evolved over the 24 h equilibration period. The volume of headspace evolved at each sampling point was estimated by measuring the amount of fluid displaced into the sampling syringe as the reactor pressure equilibrated with the atmosphere. We note that similar volumes of headspace evolved in reactors whose septa were pierced but to which no methanolic spiking solution was added. Headspace evolution, therefore, appears to be a response to the partial release of overpressure that had built up in our system over the 24 h equilibration period.

Reported aqueous concentrations of all species were corrected for volatilization losses through a calculation utilizing reported Henry's law constants and our estimates of accumulated headspace volume at each sampling point. Henry's law constants for most halogenated species (which are included in Table S-1 of the Supporting Information) were obtained from Mackay et al. (*26*); those for BCA, 1,1-DBA, ethane, and ethylene were obtained from Hine and Mookerjee (*27*), while values for *cis*-2-butene and 2-butyne were from our previous work (*24*).

For the alkyl polyhalides considered, corrections for partitioning to the headspace were of minor importance. For instance, only 5% of the total mass of 1,1,1-TCA (K_H' = 0.71 [(mol/L_{air})/(mol/L_{water})]) and less than 0.1% of the total mass of 1,1,2,2-TeCA (K_H' = 0.01) would be transferred to 10mL of evolved headspace. Such corrections were more

important in establishing mass balances for reactions that generated volatile products such as ethane and ethylene (K_H' values of 20.4 and 8.7, respectively).

When sampling had concluded, the final system pH was measured within the anaerobic chamber using a Ross combination electrode (Orion) and an Accumet AR15 pH meter (Fisher). For experiments that measured pH as a function of time, sacrificial sampling of multiple, identical batch reactors was performed.

Gas Chromatography. For systems with 1,1,1-TCA, 1,1,1,2-TeCA, 1,1,2-TCA, 1,1-DBA, and BCA, 1 mL samples were withdrawn periodically from reaction vessels while simultaneously injecting an equal volume of deoxygenated buffer at pH_0 so as to avoid introducing headspace. These samples were analyzed via static headspace gas chromatography (GC) with flame-ionization detection (FID) as described by Fennelly and Roberts (*24*). Calibration curves for most analytes were generated in a manner identical to that detailed in our previous studies (*21*, *24*). Calibration curves for ethane, ethylene, and *cis*-2-butene were generated by using an airtight syringe to add a known volume of a gas standard for each species to 1 mL of aqueous buffer within a 2 mL autosampler vial. The vial was rapidly sealed and subsequently analyzed by GC/FID.

The low K_H' values of HCA, PCA, 1,1,2,2-TeCA, and 1,2-DBA necessitated a different analytical approach. For these species, 1.5 mL of solution was removed from reaction vessels, of which 1 mL was transferred to an autosampler vial and analyzed by GC/FID as described above for quantification of volatile reduction products. Of the remaining sample, 200 μL was extracted with 2 mL of hexane, followed by subsequent dilutions in hexane. Extraction efficiencies for all species were nearly 100%. Diluted extracts were analyzed via a GC (Fisons HRGC Mega 2 series) with electron capture detection (ECD) and an RT_X-1 column (30 m × 0.32 mm i.d. × 5 μm film thickness, Restek). On-column injection (1 μL) of samples was made using an AS 800 liquid autosampler (Fisons). Standards for these analytes were prepared in hexane and were analyzed in an identical manner to the experimental samples.

Influence of Reactor Sampling on Reported Concentrations. For all species, aqueous concentrations determined from GC analyses were corrected to account for dilution from the addition of fresh buffer solution during sampling. The extent of dilution was dependent on several experimental factors, most important of which were the number and volume of aqueous samples taken during the reaction time course. In nearly all cases, this dilution correction adjusted aqueous concentrations by less than 5%.

The iron mass loading was not subject to alteration as a result of our sampling procedure. Prior to sampling, all batch reactors were placed on a magnetic stir plate to allow the iron particles to settle. This separation step allowed us to restrict our samples to the aqueous phase.

Results and Discussion

Reaction of Alkyl Polyhalides with Iron. The analyte of interest in most experiments was 1,1,1-TCA, for which an example time course is shown in Figure 1a. The observed reduction products are in accordance with our prior observations (*24*), with carbon mass balances generally greater than 85%. The slight loss of mass probably results from minor reaction products (C_3, C_5, and C_6 compounds, presumably the result of radical coupling, were identified but not quantified). It is also likely that some volatile products, specifically ethane and ethylene, were lost from batch systems via piercings in the septa used to seal the reactors.

Comparable carbon mass balances (>80%) were achieved for the other organohalides investigated. For all species,

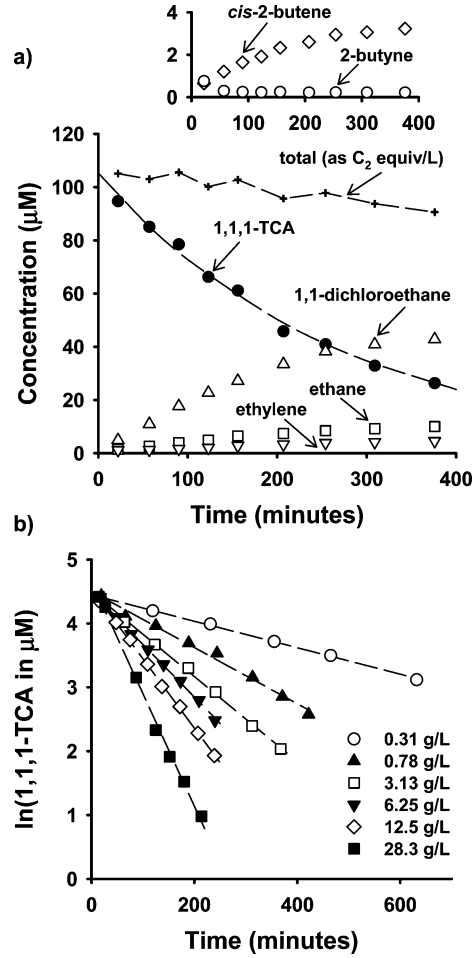

FIGURE 1. (a) Typical reaction time course for 1,1,1-TCA reduction by Fisher electrolytic iron. Reactor contains 2.5 g of iron L^{-1} and 0.1 M NaCl/0.05 M Tris buffer (pH_0 7.30) and was mixed on a jar mill at 45 rpm. Dashed line represents exponential decay fit to 1,1,1-TCA data. Inset shows trace reduction products formed. (b) Plots of the natural log of aqueous 1,1,1-TCA concentration vs time for six values of ρ_m in Tris buffer with a pH_0 of 7.30. Dashed lines represent pseudo-first-order model fits, the slopes of which were used to determine values of k_{obs}.

observed products (included in Table S-1 of the Supporting Information) were consistent with reductive dehalogenation; products indicative of other processes (such as hydrolysis of 1,1,2,2-TeCA to TCE, which may be catalyzed by the presence of a metal oxide surface (*28*)) were not observed in significant quantities (≤5% of total system mass), even though such products are relatively stable under our experimental conditions.

A pseudo-first-order kinetic model was applied to the reduction of all polyhalogenated ethanes. Values of k_{obs} were obtained from plots of the natural logarithm of alkyl polyhalide aqueous concentration versus time, such as those shown in Figure 1b for 1,1,1-TCA batch systems with six different ρ_m values. In most cases, linear regressions yielded R^2 (adjusted) values greater than 0.97, with no apparent trend to the residuals.

Influence of Reductant Mass Loading on k_{obs} for Alkyl Polyhalide Reduction. Batch experiments with 1,1,1-TCA (50 mM Tris, pH_0 7.30) revealed a nonlinear relationship between k_{obs} and ρ_m (Figure 2a) in which the rate of increase of k_{obs} decreased with increasing iron mass loading. For these systems, the reaction order in ρ_m was determined from

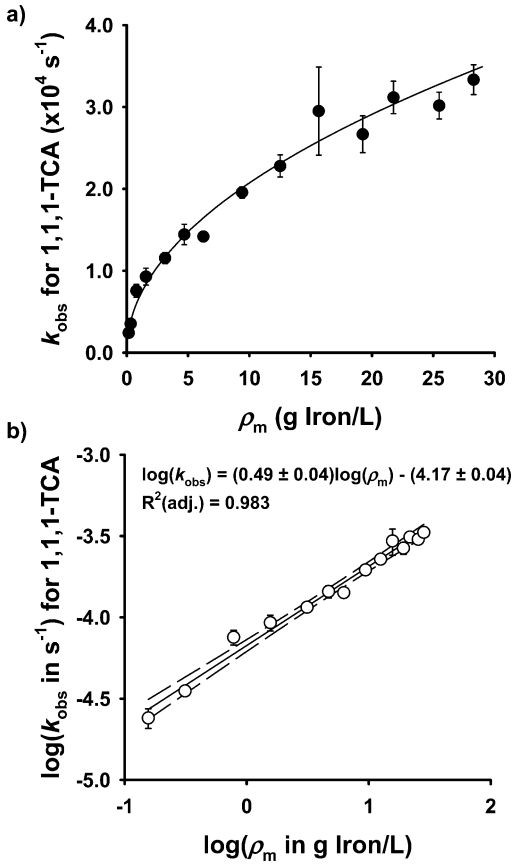

FIGURE 2. (a) Nonlinear influence of ρ_m on k_{obs} for the reduction of 1,1,1-TCA by Fisher electrolytic iron. Solid line represents fit to experimental data obtained from plots of log(k_{obs}) vs log(ρ_m). Uncertainties represent 95% confidence intervals. If no error bars are visible, then they are smaller than the symbol. Reactors contain 0.1 M NaCl/0.05 M Tris buffer (pH$_0$ 7.30). (b) Plot of log(k_{obs}) vs log(ρ_m) used to determine the reaction order in ρ_m for the data in part a. Solid line represents linear regression fit to the experimental data, while dashed lines represent 95% confidence intervals.

theslope of log(k_{obs}) versus log(ρ_m) plots according to eqs 3 and 4.

$$k_{obs} = k'(a_s\rho_m)^x \quad (3)$$

$$\log(k_{obs}) = x\log(\rho_m) + x\log(a_s) + \log(k') \quad (4)$$

In these expressions, x represents the order of reaction in ρ_m, while k' is a rate constant (with units dependent on x) equal to k_{obs} when the product of a_s and ρ_m is unity. For the data in Figure 2a, the reaction order in ρ_m was determined to be 0.49 (±0.04) (Figure 2b).

Values of k_{obs} in Figure 2a were used to calculate surface-area-normalized rate constants at each ρ_m (using an a_s of 0.4 m^2/g from Kr-BET; see eq 2). The nonlinear relationship between k_{obs} and ρ_m produces k_{SA} values that decrease with increasing ρ_m by more than an order of magnitude over the mass loadings investigated, as shown in Figure 3a. Although k_{SA} values appear to approach a lower limit at large ρ_m, a plot of log(k_{SA}) versus log(ρ_m) (Figure 3b) clearly illustrates the monotonic decrease in k_{SA} over the range of ρ_m values investigated.

Studies with most, but not all, alkyl polyhalides revealed similar nonlinear relationships. In such cases, the reaction orders in ρ_m ranged from 0.45 (±0.10) to 0.74 (±0.16) (Figure S-1 and Table S-1 in the Supporting Information). The nonlinearity was evident even though several different reduction pathways predominated, including hydrogenolysis

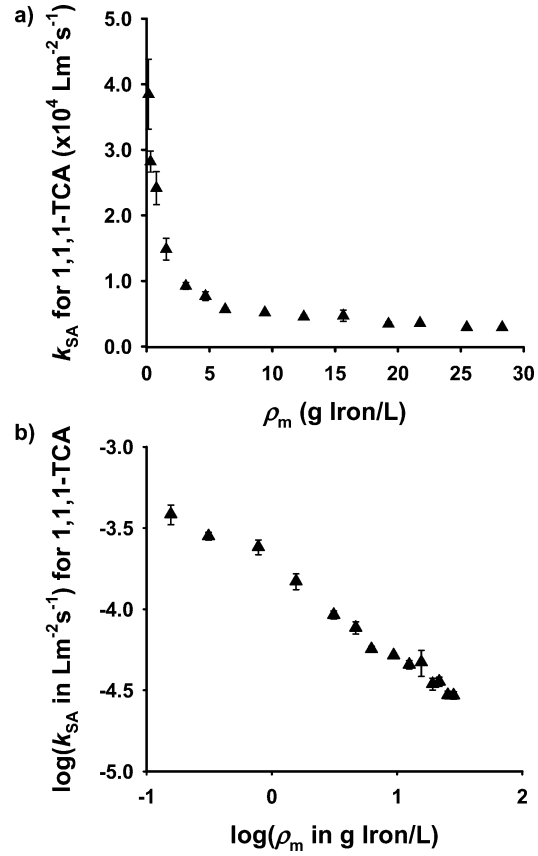

FIGURE 3. Plots of k_{SA} for 1,1,1-TCA reduction vs ρ_m on a (a) linear and (b) logarithmic scale. Data are transformed from Figure 2.

and reductive α- and β-elimination. Such a relationship is not, therefore, restricted to a particular reduction pathway or alkyl polyhalide but may be a response to the experimental conditions or the iron employed.

HCA and PCA proved exceptions (Figure 4), exhibiting a range of iron loadings (ρ_m < 3.2 g/L) over which the reaction order in ρ_m did not differ from unity (1.06 ± 0.14 and 1.07 ± 0.16, respectively). Additional experiments with PCA at higher ρ_m (3.2−9.3 g/L), however, revealed substantial deviation from linear behavior. At these elevated loadings, the reaction order in ρ_m (0.48 ± 0.12) was similar to that observed for most other alkyl polyhalides investigated.

Influence of Alkyl Polyhalide Mass Transport on Reaction Kinetics. It has been proposed (*11*) that the nonlinear relationship between k_{obs} and iron loading results from a shift from mass-transfer-limited reaction kinetics at low ρ_m to kinetics limited by rates of surface reaction at high ρ_m. As discussed by Arnold et al. (*29*), $1/k_{obs}$ for the reaction of a solute at a surface can be represented as the sum of two resistances in series

$$\frac{1}{k_{obs}} = \frac{1}{a}\left(\frac{1}{k_L} + \frac{1}{k_{SA}}\right) \quad (5)$$

where a (m^{-1}) is the ratio of metal surface area to solution volume and k_L (m s^{-1}) is the coefficient for mass transport. We note that eq 5 assumes a linear, first-order relationship between reaction rate and a (and hence ρ_m), regardless of whether kinetics are dominated by rates of alkyl polyhalide mass transport (i.e., $k_L \ll k_{SA}$) or surface reaction (i.e., $k_{SA} \ll k_L$). A changeover between mass-transfer-limited kinetics at low ρ_m and surface-reaction-limited kinetics at high ρ_m as proposed by Gotpagar et al. (*11*) would not, therefore, be anticipated from such an expression.

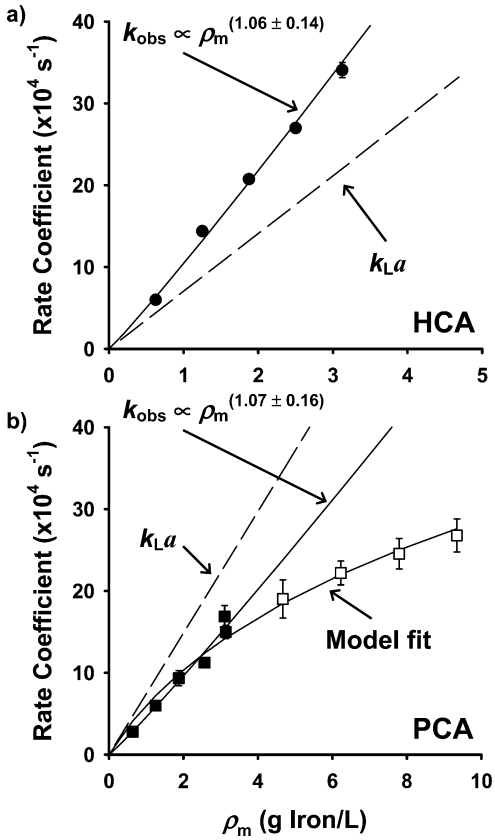

FIGURE 4. Plots of k_{obs} as a function of ρ_m for (a) HCA and (b) PCA. Reactors contain 0.1 M NaCl/0.05 M Tris buffer (pH$_0$ 7.20). Solid straight lines represent linear, first-order fits to experimental k_{obs} data obtained from plots of log(k_{obs}) vs log(ρ_m) for ρ_m < 3.2 g/L. Dashed straight lines represent estimates of the mass-transport rate coefficient (k_La) for each species as a function of ρ_m. For PCA, note the linear regime observed for ρ_m < 3.2 g/L (solid symbols) and the nonlinear regime for ρ_m > 3.2 g/L (open symbols). The solid curve in part b represents a model fit to experimental data, obtained when eq 5 of the text was modified to account for a nonlinear dependence of the surface reaction component of k_{obs} on iron loading such that $1/k_{obs} = (1/k_La + 1/k_{SA}a^x)$.

In their study of alkyl polyhalide reduction by granular zinc, Arnold et al. (*29*) successfully applied a method for estimating k_L values to batch systems that were otherwise identical to the reactors employed in this study. Proposed by Harriott (*30*), this method is based upon a semi-theoretical correlation established by Ranz and Marshall (*31*) that relates coefficients for mass transfer to and from particles suspended in solution to the diameter and settling velocity of the particles, as well as to the diffusivity of the reacting species and the kinematic viscosity of the fluid. Application of this method to our granular iron systems should provide a reasonable estimate of k_L, although some uncertainty may be expected given certain assumptions required.

This approach requires that a in eq 5 be expressed on the basis of geometric surface area ($a = (4\pi r_p^2)/$(solution volume)) rather than being computed from Kr-BET surface area. For our Fisher iron, the surface area of 0.4 m^2/g from Kr-BET is ~80 times larger than the geometric surface area calculated assuming our particles are uniform spheres with a radius (r_p) of 75 μm (consistent with 100 mesh particles). This difference either reflects a nonuniform particle size distribution or indicates that our iron contains substantial "internal" surface area potentially subject to additional mass-transfer resistance (*29*) (which will not be considered here). Consequently, the use of geometric surface area will introduce some uncertainty into our estimates of k_La values. Furthermore, our estimation technique assumes that the particle surface is of a relatively uniform reactivity, and additional uncertainty may result if the fraction of the geometric surface area that is redox-active is less than unity. Comparisons of k_La to k_{obs}, therefore, should only be interpreted as possible evidence of mass-transfer limitations; a more definitive indication would be if faster rates of reduction could not be achieved in analogous experimental systems even with inherently more reactive oxidants that possess similar diffusivities.

Estimates of k_La suggest that the reduction of 1,1,1-TCA, 1,2-DBA, 1,1,2,2-TeCA, 1,1,2-TCA, and BCA is not likely limited by mass transfer. For example, computed values of $1/(k_La)$ for 1,1,1-TCA were generally less than 10% of $1/k_{obs}$ at each ρ_m considered for pH$_0$ 7.20 and 7.30 (for comparison of estimated k_La to experimental k_{obs} values for select species, see Figure S-2 of the Supporting Information). The same cannot be said for 1,1,1,2-TeCA and 1,1-DBA, for which $1/(k_La)$ was as much as 30% and 55% of $1/k_{obs}$, respectively. Similarly, estimates of $1/(k_La)$ for PCA were on average nearly 65% of $1/k_{obs}$ for ρ_m < 3.2 g/L, while $1/(k_La)$ estimates for HCA were roughly a factor of 1.5 *greater* than the measured $1/k_{obs}$ (Figure 4).

The substantive contribution of $1/(k_La)$ to $1/k_{obs}$ for 1,1-DBA, 1,1,1,2-TeCA, PCA, and HCA suggests that reduction of these species could be at least partially limited by mass transport. More importantly, we have been unable to achieve greater k_{obs} values than those reported herein for HCA, even in systems with bimetallic reductants (Ni/Fe and Pd/Fe) generated from Fisher electrolytic iron that exhibit increased reactivity toward other alkyl polyhalides (data not shown). We hypothesize, therefore, that the linear relationships between k_{obs} and ρ_m observed for HCA and PCA (for ρ_m < 3.2 g/L) result from reduction kinetics limited by rates of organohalide transport to the iron surface ($k_{obs} \approx k_La$). Moreover, the contribution of $1/(k_La)$ to $1/k_{obs}$ for 1,1-DBA and 1,1,1,2-TeCA likely results in the somewhat greater reaction orders in ρ_m observed for these species relative to most of the other alkyl polyhalides investigated.

Given the similar aqueous diffusivities of PCA and HCA (7.2×10^{-6} and 6.6×10^{-6} cm^2/s, respectively, estimated by the method of Wilke and Chang (*32*)), our estimates of k_La are nearly identical for these species. If our assumption of mass transfer control is correct, then the 2-fold difference between experimental k_{obs} values for HCA and PCA reduction at a given ρ_m (compare Figures 4a and 4b) suggests that estimates of k_La for our Fisher electrolytic iron batch systems are likely within a factor of 2 of their actual value. This level of agreement is quite good considering the numerous approximations required by this estimation technique.

We propose that the nonlinearity observed at ρ_m > 3.2 g/L for PCA indicates a shift to a regime at which rates of surface reaction predominate. This is supported by our ability to successfully model k_{obs} for PCA over the entire range of ρ_m when the surface reaction component of eq 5 is modified to account for a nonlinear dependence on iron loading (i.e., $1/k_{obs} = (1/k_La + 1/k_{SA}a^x)$; Figure 4b). Such behavior, however, does not provide any insight as to why the rate of surface reaction does not vary linearly with a and hence ρ_m.

Influence of Experimental Variables on k_{obs} versus ρ_m. A nonlinear relationship between k_{obs} and ρ_m was observed for the reaction of 1,1,1-TCA under all experimental conditions investigated. For instance, it was noted with each mixing apparatus, mixing speed, and buffer solution employed in this study. Such a relationship was also obtained for reactors to which 1,1,1-TCA was added immediately after reactor construction rather than after a 24 h equilibration period. Values of k_{obs} also proved independent of the initial 1,1,1-TCA concentration over the range investigated (5−200 μM), suggesting that a combined zero- and first-order model such as the one employed by Wüst et al. (*13*) cannot entirely explain

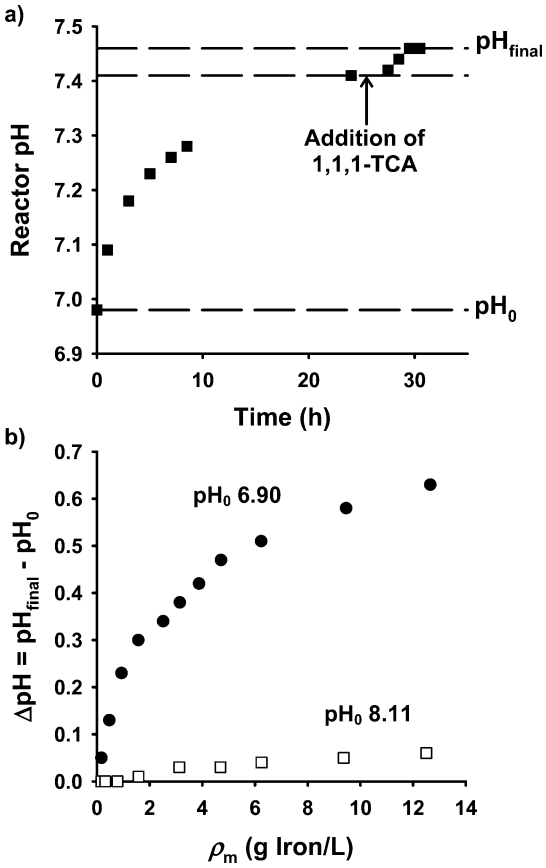

FIGURE 5. (a) Plot of reactor pH as a function of time in a batch system with 6.3 g of iron L^{-1} and 0.1 M NaCl/0.05 M Tris (pH_0 6.98). The majority of the pH increase occurs prior to the addition of 1,1,1-TCA to the reactor (indicated by the arrow at $t \approx 24$ h). (b) Change in reactor pH (ΔpH) as a function of ρ_m for systems with an initial pH of 6.90 and 8.11.

the nonlinear relationship. A more detailed discussion of these results (summarized in Figures S-3 through S-7) can be found in the Supporting Information.

One noteworthy variable was the system pH. Despite the presence of 50 mM buffer, the pH increased substantially over the lifetime of most reactors, presumably the result of proton ($2H^+ + 2e^- \rightarrow H_2$) and water ($2H_2O + 2e^- \rightarrow H_2 + 2OH^-$) reduction at the iron surface (*33*). For example, in a reactor with 6.3 g/L iron and 50 mM Tris (pH_0 6.98), the system pH increased by 0.48 pH units from the time of reactor assembly (at $t = 0$) until the conclusion of the reaction with 1,1,1-TCA ($t \approx 30$ h) (Figure 5a). Most of this change (0.43 pH units) occurred over the 24 h prior to 1,1,1-TCA addition, while the solution pH was nearly constant during the actual reaction. As a result, the system pH during 1,1,1-TCA reduction is best approximated by pH_{final}, the pH measured at the *conclusion* of our experiments. We also note that the magnitude of this pH change ($\Delta pH = pH_{final} - pH_0$) increased with increasing ρ_m and was greater at lower pH_0 (e.g., 6.90) than at higher pH_0 (e.g., 8.11; see Figure 5b).

For a given ρ_m, k_{obs} for 1,1,1-TCA reduction decreased with increasing pH_{final} (Figure 6), consistent with previously reported dependencies of granular iron reactivity on solution pH (*1*, *34*). Interestingly, the relationships between k_{obs} and pH_{final} shown in Figure 6 reveal a pronounced dependence on the value of ρ_m considered. For instance, values of k_{obs} measured at low iron loadings (0.2 g/L) were fairly insensitive to changes in pH_{final}, while values of k_{obs} measured at higher ρ_m (1.6 and 6.3 g/L) decreased substantially with increasing pH_{final}.

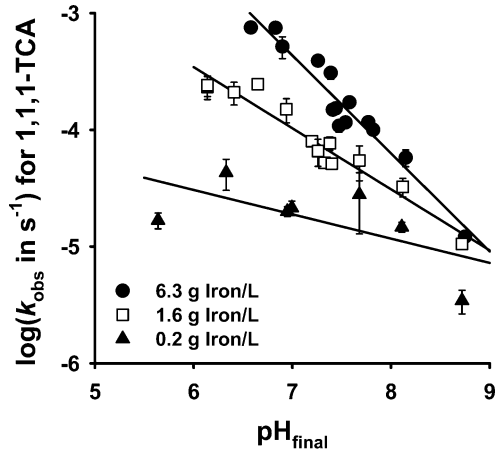

6.3 g Iron/L
$\log(k_{obs}) = -(0.84 \pm 0.14) \times pH_{final} + (2.5 \pm 1.0)$
R^2(adj.) = 0.929, n = 14

1.6 g Iron/L
$\log(k_{obs}) = -(0.52 \pm 0.09) \times pH_{final} - (0.32 \pm 0.66)$
R^2(adj.) = 0.930, n = 13

0.2 g Iron/L
$\log(k_{obs}) = -(0.21 \pm 0.29) \times pH_{final} - (3.2 \pm 2.1)$
R^2(adj.) = 0.291, n = 7

FIGURE 6. Dependence of $\log(k_{obs})$ for 1,1,1-TCA reduction on pH_{final} for three values of ρ_m (0.2, 1.6, and 6.3 g/L). Experiments were conducted in 0.1 M NaCl and either 0.05 M MES (pH_0 5.50−6.50) or 0.05 M Tris (pH_0 6.90−8.65). Solid lines represent best-fit linear regressions to the experimental data, as indicated for each loading. The low R^2 (adjusted) value obtained at a ρ_m of 0.2 g/L results from the near independence of k_{obs} on pH_{final} at this iron loading.

As iron reactivity decreases with increasing pH_{final}, it might be tempting to infer that the nonlinear relationship between k_{obs} and ρ_m stems from the influence of ρ_m on ΔpH (Figure 5b). Specifically, one might question whether k_{obs} values measured in systems with large ρ_m can be directly compared to k_{obs} values measured at low ρ_m, owing to systematic reactor-to-reactor differences in solution pH during the time interval when k_{obs} values are measured. The higher pH_{final} encountered in systems with large ρ_m would work to depress iron reactivity and could potentially be responsible for our observation that k_{obs} values do not scale in a linear, first-order manner with increasing ρ_m.

To explore whether variations in ΔpH with ρ_m were of sufficient magnitude to explain the nonlinearity between k_{obs} and ρ_m, we estimated k_{obs} values for 1,1,1-TCA reduction that might have been measured had the system pH remained fixed at pH_0 for all ρ_m. As shown in eq 6, estimates of k_{obs} at pH_0 were calculated using the slopes (m) of the linear relationships shown in Figure 6 to adjust experimental k_{obs} values (measured at pH_{final}) to account for changes in reactivity resulting from ΔpH at the three loadings considered (i = 0.2, 1.6 and 6.3 g/L).

$$\log(k_{obs})_{pH_0,i} = \log(k_{obs})_{pH_{final},i} - (\Delta pH_i m_i) \qquad (6)$$

When performed on k_{obs} data for 1,1,1-TCA reduction at a pH_0 of 6.90, this correction does indeed increase the linearity between k_{obs} and ρ_m (solid symbols and dashed line in Figure 7a). The reaction order in ρ_m for these ΔpH-adjusted k_{obs} data is approximately 0.8, which given the uncertainty in the correction procedure is likely not significantly different from unity. When applied to k_{obs} data at a pH_0 of 8.11, however, this correction results in a negligible increase in k_{obs} and a relationship between k_{obs} and ρ_m that remains decidedly nonlinear (Figure 7b). The reaction order in ρ_m for these

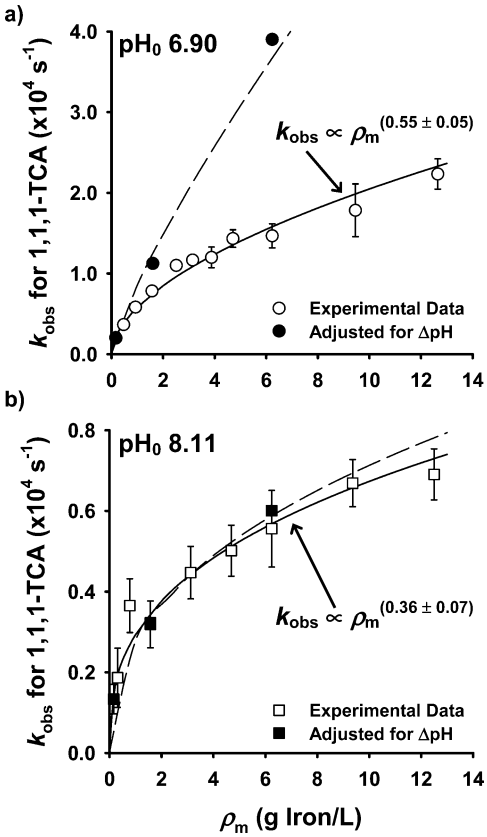

FIGURE 7. Plots of k_{obs} for 1,1,1-TCA reduction as a function of ρ_m for batch experiments conducted in 0.1 M NaCl/0.05 M Tris buffer with pH_0 of (a) 6.90 and (b) 8.11. Solid lines represent fits to experimental data (open symbols) obtained from plots of log(k_{obs}) vs log(ρ_m). Solid symbols represent values of k_{obs} at ρ_m values of 0.2, 1.6, and 6.3 g/L that have been adjusted to account for changes in system pH using the relationships from Figure 6. Dashed lines represent fits to these adjusted k_{obs} values, obtained from plots of log(k_{obs}) vs log(ρ_m) for the ΔpH-adjusted data.

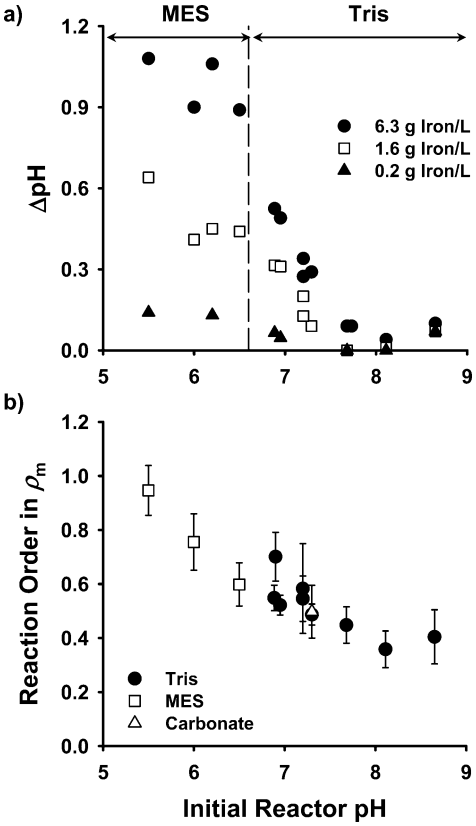

FIGURE 8. (a) Plot of ΔpH as a function of pH_0 for batch systems examining the reduction of 1,1,1-TCA at three different values of ρ_m. Dashed vertical line separates ΔpH data collected in 0.05 M MES buffer systems from those collected in 0.05 M Tris buffer systems. All systems contained 0.1 M NaCl. (b) Plot of the reaction order in ρ_m as a function of pH_0 for the reduction of 1,1,1-TCA in Tris (solid circles), MES (open squares), and carbonate (open triangles) buffer systems.

adjusted data is approximately 0.4, a value not statistically different from that obtained with the uncorrected k_{obs} data (0.36 ± 0.07). Moreover, applying this correction to data obtained at pH_0 5.50 produces a relationship between k_{obs} and ρ_m that is again nonlinear, but this time with a reaction order in ρ_m in excess of unity (~1.5). Our results suggest, therefore, that while differences in ΔpH with ρ_m could certainly influence the degree of nonlinearity between k_{obs} and ρ_m, such differences cannot entirely or invariably account for the nonlinear behavior.

If the observed nonlinearity were to predominantly reflect pH changes that occurred prior to the reaction between iron and 1,1,1-TCA, then one might anticipate a smaller order in ρ_m for systems with low values of pH_0, which yielded the largest ΔpH values at each iron loading considered (Figure 8a). Yet our experimental data reveal the opposite trend; the reaction order in ρ_m clearly decreases with pH_0 (Figure 8b). In fact, a pH_0 of 5.50 yielded a reaction order indistinguishable from unity (0.95 ± 0.09). We note that k_{obs} values for these systems were 6-fold less than estimates of k_La for 1,1,1-TCA (Figure S-2b in the Supporting Information) and were on average 3.5-fold less than the k_{obs} values measured for PCA at a similar ρ_m (Figure 4b). We also note that these k_{obs} values for 1,1,1-TCA reduction are a factor of 3 less than the k_{obs} values for 1,1-DBA reduction that yielded a reaction order in ρ_m of 0.74 ± 0.16. We therefore maintain that the reaction order of 0.95 ± 0.09 obtained for 1,1,1-TCA at pH_0 5.50 is unlikely to reflect the onset of mass-transfer control.

Link between k_{obs} and Rates of Iron Corrosion. The similar dependencies of ΔpH and k_{obs} on ρ_m (compare Figures 5b and 7) suggest that the magnitude of ΔpH may be closely linked to granular iron reactivity toward alkyl polyhalides. The concentration of reduced protons and water resulting in ΔpH at each ρ_m, therefore, may provide a useful metric of the redox activity of granular iron.

We can estimate this value via a mass balance on protons (eq 7), recognizing that every mole of protons or water reduced increases system pH.

$$[H_{red}] = ([HA]_0 - [HA]_t) - ([H^+]_t - [H^+]_0) \qquad (7)$$

In eq 7, $[H_{red}]$ is the summed concentration of protons and water reduced by iron over the interval from $t = 0$ to some later time t. The value of t chosen for all calculations was 24 h, corresponding to the time immediately prior to the addition of organohalide to our batch systems. [HA] represents the concentration of the buffer in its protonated form, while $[H^+]$ is the aqueous concentration of protons. Both [HA] and $[H^+]$ at $t = 0$ and 24 h can be calculated from the total concentration (50 mM) and acid dissociation constant of the pH buffer, in addition to our measurements of system pH. Essentially, eq 7 estimates the concentration of protons and water reduced at each ρ_m over a 24 h period by calculating the difference in aqueous-phase proton concentration at $t = 0$ and $t = 24$ h, while also accounting for the release of H^+(aq) by the pH buffer during this interval.

If we apply eq 7 to Tris ($pK_a = 8.1$) buffer systems with a pH_0 of 6.90, then estimates of $[H_{red}]$ range between 0.3 and

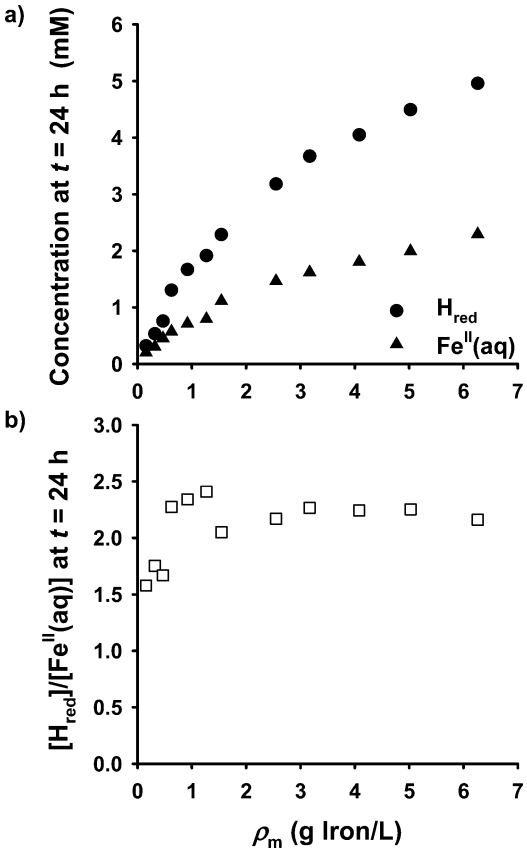

FIGURE 9. (a) Plots of H_{red} (circles) and $Fe^{II}(aq)$ (triangles) concentration as a function of ρ_m for systems with 0.1 M NaCl/0.05 M Tris (pH_0 6.90). Concentrations were quantified 24 h after reactor assembly (immediately prior to addition of 1,1,1-TCA). (b) Ratio of $[H_{red}]$ to $[Fe^{II}(aq)]$ as a function of ρ_m in samples analyzed 24 h after reactor assembly.

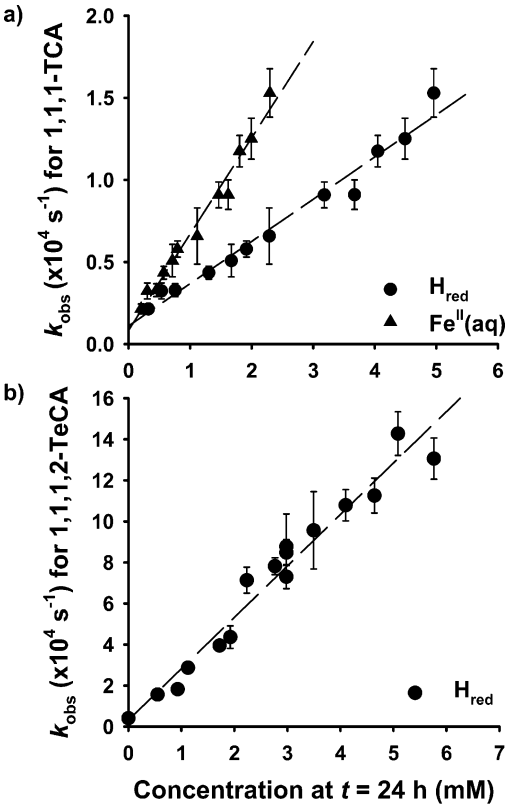

FIGURE 10. (a) Linear correlations between k_{obs} for 1,1,1-TCA reduction and values of $[H_{red}]$ and $[Fe^{II}(aq)]$ from Figure 9a. Dashed lines represent linear regression fits to the experimental data. (b) Linear correlation between k_{obs} for 1,1,1,2-TeCA reduction and $[H_{red}]$. All experiments were conducted in batch systems containing 0.1 M NaCl/0.05 M Tris buffer (pH_0 6.90 for 1,1,1-TCA; pH_0 7.50 for 1,1,1,2-TeCA).

5.0 mM for the ρ_m investigated (Figure 9a). For these same systems, concentrations of aqueous Fe^{II} species generated over 24 h range between 0.2 and 2.3 mM (Figure 9a). These concentrations are below the solubility limit for Fe^{II} established by $Fe(OH)_2(s)$ formation ($Fe(OH)_2(s) = Fe^{2+} + 2OH^-$; $\log(K_{sp}) = -15.1$) (*35*). Interestingly, both $[H_{red}]$ and $[Fe^{II}(aq)]$ increased in a nonlinear fashion with respect to ρ_m in a manner similar to that observed for k_{obs} for 1,1,1-TCA reduction (compare Figures 7 and 9a). Furthermore, the ratio of $[H_{red}]$ to $[Fe^{II}(aq)]$ was nearly 2 for most iron loadings (Figure 9b), although it was somewhat smaller at low ρ_m, likely reflecting difficulties in accurately determining ΔpH (often <0.1 pH units at low ρ_m). We emphasize that these concentrations of H_{red} and $Fe^{II}(aq)$ were generated prior to the addition of 1,1,1-TCA to reactors and in the case of $Fe^{II}(aq)$ are much larger than concentrations anticipated (~160 μM) if the reduction of 1,1,1-TCA to the observed products was solely responsible for $Fe^{II}(aq)$ production.

If we correlate k_{obs} for 1,1,1-TCA reduction at each ρ_m to the values of $[H_{red}]$ and $[Fe^{II}(aq)]$ generated over 24 h at that same ρ_m, then linear relationships are observed (Figure 10a). Similar relationships were encountered for 1,1,1-TCA at other pH_0 values as well as for other alkyl polyhalides investigated, as the data in Figure 10b reveal for 1,1,1,2-TeCA. Note that 1,1,1,2-TeCA reacts entirely via reductive β-elimination to produce 1,1-dichloroethylene. The existence of a linear relationship between $[H_{red}]$ and k_{obs} for 1,1,1,2-TeCA, a species reacting entirely via electron transfer, indicates that reactivity correlations with $[H_{red}]$ are not limited to species that react predominantly via a hydrogen-incorporating reduction pathway (e.g., hydrogenolysis).

These linear correlations invite the speculation that some form of reduced hydrogen or Fe^{II} could represent the entity responsible for alkyl polyhalide reduction. In fact, several researchers have proposed either surface-associated atomic hydrogen (*36*−*39*) or surface-adsorbed Fe^{II} (*1*, *40*) as the reactive moiety in granular iron systems. As nearly all H_{red} and $Fe^{II}(aq)$ is generated prior to the contact of iron with the organohalide, however, we do not believe their relationship to k_{obs} necessitates their direct involvement in polyhalogenated ethane reduction. Moreover, while H_{red} and $Fe^{II}(aq)$ accumulate in batch systems over time, iron reactivity decreases (Figure S-6 in the Supporting Information), behavior counter to expectations if either species were directly linked to alkyl polyhalide reduction. Finally, we maintain that important differences must exist between surface-associated Fe^{II} in iron oxide suspensions and Fe^{II} as a reactive entity in granular iron systems. Specifically, the reactivity of the former has been shown to increase with pH (*41*), while our studies and those of others clearly demonstrate that granular iron reactivity decreases with pH.

Mechanistic Insights from Linear Reactivity Correlations. Both $[H_{red}]$ and $[Fe^{II}(aq)]$ are time-dependent concentrations produced from the reduction of protons/water by granular iron. Values of $[H_{red}]$ and $[Fe^{II}(aq)]$ determined at a point in time, therefore, represent a measure of the *rate* of proton/water reduction at each ρ_m that in turn can be presumed to be proportional to the total number of reactive sites on the iron surface responsible for proton/water reduction. We propose that the linear correlations between $[H_{red}]$, $[Fe^{II}(aq)]$, and k_{obs} for alkyl polyhalide reduction could reflect a link between the sites at which proton/water reduction occurs and the surface species responsible for alkyl

polyhalide reduction. Such a link was suggested previously by Deng et al. (*42*) from batch studies, in which a close correlation was observed between rates of H_2(g) production and rates of TCE reduction by granular iron.

These linear correlations, and the 2:1 stoichiometry of [H_{red}] to [Fe^{II}(aq)] might lead one to suggest that metallic iron is the responsible entity in both proton/water and alkyl polyhalide reduction. We note, however, that the half-reaction for magnetite oxidation to maghemite (*43*), when coupled with the half-reactions for proton and water reduction, also produces a 2:1 stoichiometry between [Fe^{II}(aq)] and [H_{red}]. We therefore cannot entirely rule out the possibility that these relationships between k_{obs} for alkyl polyhalide reduction and [Fe^{II}(aq)] or [H_{red}] implicate magnetite, a corrosion byproduct observed in granular iron systems (*44*) that is capable of reducing organohalides (*45*), as the redox-active entity in our batch systems.

Implications of a Nonlinear Relationship between k_{obs} and ρ_m. The nonlinear relationship between k_{obs} and ρ_m indicates that granular iron reactivity decreases with increasing iron loading in our batch systems. Although one might interpret this behavior as evidence that the fraction of the total iron surface area that is redox-active decreases with increasing loading, we do not consider our results to be entirely consistent with this scenario. Specifically, if reactive surface area were to decrease with increasing ρ_m (such that the effective a in eq 5 did not vary linearly with ρ_m), then we would anticipate a nonlinear relationship between k_{obs} and ρ_m even under mass-transfer-limited conditions. Instead, a linear, first-order relationship between k_{obs} and ρ_m was observed for HCA and PCA reduction at iron loadings less than 3.2 g/L. We suggest these linear relationships are evidence that the fraction of total iron surface area that is redox-active is fairly constant over the range of ρ_m investigated in this study.

Rather, it appears that the inherent reactivity of our granular iron particles changes with iron mass loading. In relating k_{obs} to ρ_m (eq 3) we have assumed that k' is independent of ρ_m. If the magnitude of k' were to decrease with increasing iron loading, then a nonlinear relationship between k_{obs} and ρ_m might still be encountered even if the fractional reactive surface area was constant for all ρ_m. For such a case, our expression for k_{obs} can be modified to the following

$$k_{obs} = k'' a_s \rho_m \tag{8}$$

where k'' is not constant but rather decreases with increasing ρ_m.

At present, the exact nature of the process that deactivates the iron surface (toward reduction of alkyl polyhalides and protons or water alike) with increasing ρ_m remains somewhat unclear. One observation that allows us to speculate on this issue is that k_{obs} becomes nearly linearly dependent on ρ_m as pH_0 decreases (Figure 8b and Figure S-7 of the Supporting Information), suggesting that surface passivation is less pronounced at low pH. At low pH, dissolution of surface-associated Fe^{II} or Fe^{III} species at anodic sites on the particle surface is likely enhanced, and hence the thickness of the oxide overlayer on iron may be minimized. At higher pH, rates of oxide dissolution should be depressed, resulting in a thicker oxide overlayer. Such an overlayer could potentially inhibit granular iron reactivity by hindering electron conduction from the metallic iron core to the particle−solution interface. We note that this scenario would still allow for a linear, first-order relationship between k_{obs} and ρ_m under mass-transfer-limited conditions, while also providing a nonlinear relationship as soon as particle reactivity decreased to the point that $1/k_{obs}$ was no longer dominated by $1/k_La$.

Why such passivation would be more pronounced in systems with larger ρ_m remains an intriguing question. Our measurements of Fe^{II}(aq) (Figure 9a) concentration and bulk solution pH at each value of ρ_m indicate that we are below the solubility limit of $Fe(OH)_2$(s), which could serve as a passivating surface oxide. We cannot rule out the possibility, however, that regions of elevated pH exist on the iron particle surface near strongly reducing sites such as corrosion pits. At these locations, the solubility of $Fe(OH)_2$(s) may be exceeded, resulting in the formation or thickening of a passivating layer. In such a scenario, it would not be unreasonable for $Fe(OH)_2$(s) formation to be greatest in systems with large ρ_m, as the bulk pH and Fe^{II}(aq) concentrations measured in these systems provide conditions that more closely approach the solubility limit for $Fe(OH)_2$(s) than measurements of the bulk pH and Fe^{II}(aq) concentrations at low iron loadings.

We stress that such a hypothesis requires experimental validation. Initial experiments in which 12.5 mM exogenous Fe^{II}(aq) was added to batch systems containing granular iron had no appreciable effect on k_{obs} relative to rate constants measured in systems free of exogenous Fe^{II}(aq) (Figure S-8 of the Supporting Information). This result appears contradictory to that expected if passivation resulting from Fe^{II} oxide formation were indeed contributing to the nonlinear relationship between k_{obs} and ρ_m. Such unresolved questions provide interesting avenues for future research into granular iron systems.

Finally, we place our results into the context of previous investigations with granular iron. To do so, values of ρ_m and k_{obs} from Table 4 of Matheson and Tratnyek (*1*) were transformed on a log−log scale to determine the reaction order in ρ_m for CCl_4 reduction in unbuffered granular iron systems. Although the relationship between iron mass loading and k_{obs} for these data certainly appears linear (*1*), we find the reaction order in ρ_m is 0.68 (±0.12). Interestingly, Fisher electrolytic iron was the metal reductant used in this prior study as well as in the current investigation. Furthermore, additional studies with Fisher iron investigating CCl_4 (*10*), *cis*-dichloroethylene (*2*), and nitrate (*6*) reduction have also produced a nonlinear relationship between k_{obs} and ρ_m. It appears, therefore, that the nonlinear dependence of k_{obs} on ρ_m may be a result generally applicable to batch studies with Fisher iron under appropriate (non-mass-transfer-limited) experimental conditions, although extension of these findings to other types of iron or to bimetallic systems will require additional investigation. Regardless of their general applicability to other zero-valent metal systems, however, our results clearly illustrate that k_{SA} values should only be applied to granular iron systems for which a relationship between k_{obs} and ρ_m has been verified to be truly first-order.

Acknowledgments

This research was funded by the U. S. Environmental Protection Agency (EPA) STAR program (Grant No. R82816401). Additional funding for D.M.C. was provided through a National Science Foundation (NSF) Graduate Research Fellowship and a U. S. EPA STAR Graduate Fellowship. The contents of this publication are the sole responsibility of the authors and do not necessarily reflect the official view of the NSF or the U. S. EPA. We are especially grateful for the efforts of five anonymous reviewers, whose insightful comments greatly improved this manuscript.

Supporting Information Available

Plots of log(k_{obs}) versus log(ρ_m), experimental reaction orders in ρ_m and reduction products for all alkyl polyhalides investigated, comparison of estimated k_La values and experimental k_{obs} values for select alkyl polyhalides, and the influence of experimental variables including mixing ap-

paratus and mixing speed, buffer composition, initial 1,1,1-TCA concentration, reactor equilibration period, pH_0, and exogenous $Fe^{II}(aq)$ on k_{obs} for 1,1,1-TCA reduction as a function of ρ_m. This material is available free of charge via the Internet at http://pubs.acs.org.

Literature Cited

(1) Matheson, L. J.; Tratnyek, P. G. Reductive dehalogenation of chlorinated methanes by iron metal. *Environ. Sci. Technol.* **1994**, *28*, 2045−2053.
(2) Arnold, W. A.; Roberts, A. L. Pathways and kinetics of chlorinated ethylene and chlorinated acetylene reaction with Fe(0) particles. *Environ. Sci. Technol.* **2000**, *34*, 1794−1805.
(3) Johnson, T. L.; Scherer, M. M.; Tratnyek, P. G. Kinetics of halogenated organic compound degradation by iron metal. *Environ. Sci. Technol.* **1996**, *30*, 2634−2640.
(4) Agrawal, A.; Tratnyek, P. G. Reduction of nitro aromatic compounds by zero-valent iron metal. *Environ. Sci. Technol.* **1996**, *30*, 153−160.
(5) Rajagopal, V.; Burris, D. R. Reduction of 1,2-dibromoethane in the presence of zero-valent iron. *Environ. Toxicol. Chem.* **1999**, *18*, 1779−1782.
(6) Alowitz, M. J.; Scherer, M. M. Kinetics of nitrate, nitrite and Cr(VI) reduction by iron metal. *Environ. Sci. Technol.* **2002**, *36*, 299−306.
(7) Huang, Y. H.; Zhang, T. C. Kinetics of nitrate reduction by iron at near neutral pH. *J. Environ. Eng.* **2002**, *128*, 604−611.
(8) Zhang, L.; Arnold, W. A.; Hozalski, R. M. Kinetics of haloacetic acid reactions with Fe(0). *Environ. Sci. Technol.* **2004**, *38*, 6881−6889.
(9) Bandstra, J. Z.; Miehr, R.; Johnson, R. L.; Tratnyek, P. G. Reduction of 2,4,6-trinitrotoluene by iron metal: kinetic controls on product distributions in batch experiments. *Environ. Sci. Technol.* **2005**, *39*, 230−238.
(10) Scherer, M. M.; Tratnyek, P. G. Dechlorination of Carbon Tetrachloride by Iron Metal: Effect of Reactant Concentrations. In *Preprints of Extended Abstracts of the Division of Environmental Chemistry*, Proceedings of the 209th National Meeting of the American Chemical Society, Anaheim, CA, 1995; American Chemical Society: Washington, DC, 1995; Vol. 35, pp 805−806.
(11) Gotpagar, J.; Gulke, E.; Tsang, T.; Bhattacharyya, D. Reductive dehalogenation of trichloroethylene using zero-valent iron. *Environ. Prog.* **1997**, *16*, 137−143.
(12) Arnold, W. A. Kinetics and Pathways of Chlorinated Ethylene and Chlorinated Ethane Reaction with Zero-Valent Metals. Ph.D. Thesis, Johns Hopkins University, Baltimore, MD, 1999.
(13) Wüst, W. F.; Köber, R.; Schlicker, O.; Dahmke, A. Combined zero- and first-order kinetic model of the degradation of TCE and *cis*-DCE with commercial iron. *Environ. Sci. Technol.* **1999**, *33*, 4304−4309.
(14) Choe, S.; Chang, Y.-Y.; Hwang, K.-Y.; Khim, J. Kinetics of reductive denitrification by nanoscale zero-valent iron. *Chemosphere* **2000**, *41*, 1307−1311.
(15) Doong, R.-A.; Chen, K.-T.; Tsai, H.-C. Reductive dechlorination of carbon tetrachloride and tetrachloroethylene by zerovalent silicon−iron reductants. *Environ. Sci. Technol.* **2003**, *37*, 2575−2581.
(16) Zhang, W.; Wang, C.-B.; Lien, H.-L. Treatment of chlorinated organic contaminants with nanoscale bimetallic particles. *Catal. Today* **1998**, *40*, 387−395.
(17) Lien, H.-L.; Zhang, W. Transformation of chlorinated methanes by nanoscale iron particles. *J. Environ. Eng.* **1999**, *125*, 1042−1047.
(18) Lien, H.-L.; Zhang, W. Nanoscale iron particles for complete reduction of chlorinated ethenes. *Colloids Surf., A* **2001**, *191*, 97−105.
(19) Nurmi, J. T.; Tratnyek, P. G.; Sarathy, V.; Baer, D. R.; Amonette, J. E.; Pecher, K.; Wang, C.; Linehan, J. C.; Matson, D. W.; Penn, R. L.; Driessen, M. D. Characterization and properties of metallic iron nanoparticles: spectroscopy, electrochemistry and kinetics. *Environ. Sci. Technol.* **2005**, *39*, 1221−1230.
(20) Scherer, M. M.; Balko, B. A.; Gallagher, D. A.; Tratnyek, P. G. Correlation analysis of rate constants for dechlorination by zero-valent iron. *Environ. Sci. Technol.* **1998**, *32*, 3026−3033.
(21) Arnold, W. A.; Roberts, A. L. Pathways of chlorinated ethylene and chlorinated acetylene reaction with Zn(0). *Environ. Sci. Technol.* **1998**, *32*, 3017−3025.
(22) Miehr, R.; Tratnyek, P. G.; Bandstra, J. Z.; Scherer, M. M.; Alowitz, M. J.; Bylaska, E. J. Diversity of contaminant reduction reactions by zerovalent iron: role of the reductate. *Environ. Sci. Technol.* **2004**, *38*, 139−147.
(23) Tratnyek, P. G.; Scherer, M. M.; Johnson, T. L.; Matheson, L. J. Permeable Reactive Barriers of Iron and Other Zero-Valent Metals. In *Chemical Degradation Methods for Wastes and Pollutants*; Tarr, M. A., Ed.; Marcel Dekker: New York, 2003; pp 371−421.
(24) Fennelly, J. P.; Roberts, A. L. Reaction of 1,1,1-trichloroethane with zero-valent metals and bimetallic reductants. *Environ. Sci. Technol.* **1998**, *32*, 1980−1988.
(25) Stookey, L. L. Ferrozine—a new spectrophotometric reagent for iron. *Anal. Chem.* **1970**, *42*, 779−781.
(26) Mackay, D.; Shiu, W. Y.; Ma, K. C. *Illustrated Handbook of Physical-Chemical Properties and Environmental Fate for Organic Chemicals*; Lewis Publishers: Chelsea, MI, 1993; Vol. 3.
(27) Hine, J.; Mookerjee, P. K. The intrinsic hydrophilic character of organic compounds. Correlations in terms of structural contributions. *J. Org. Chem.* **1975**, *40*, 292−298.
(28) Arnold, W. A.; Winget, P.; Cramer, C. J. Reductive dechlorination of 1,1,2,2-tetrachloroethane. *Environ. Sci. Technol.* **2002**, *36*, 3536−3541.
(29) Arnold, W. A.; Ball, W. P.; Roberts, A. L. Polychlorinated ethane reaction with zero-valent zinc: pathways and rate control. *J. Contam. Hydrol.* **1999**, *40*, 183−200.
(30) Harriott, P. Mass transfer to particles suspended in agitated tanks. *AIChE J.* **1962**, *8*, 93−102.
(31) Ranz, W. E.; Marshall, W. R. Evaporation from drops. *Chem. Eng. Prog.* **1952**, *48*, 141−146.
(32) Wilke, C. R.; Chang, P. Correlation of diffusion coefficients in dilute solution. *AIChE J.* **1955**, *1*, 264−270.
(33) Reardon, E. J. Anaerobic corrosion of granular iron: measurement and interpretation of hydrogen evolution rates. *Environ. Sci. Technol.* **1995**, *29*, 2936−2945.
(34) Támara, M. L.; Butler, E. B. Effects of iron purity and groundwater characteristics on rates and products in the degradation of carbon tetrachloride by iron metal. *Environ. Sci. Technol.* **2004**, *38*, 1866−1876.
(35) Smith, R. M.; Martell, A. E. *Critical Stability Constants: Inorganic Complexes*; Plenum: New York, 1976.
(36) Odziemkowski, M. S.; Gui, L.; Gillham, R. W. Reduction of *N*-nitrosodimethylamine with granular iron and nickel-enhanced iron. 2. Mechanistic studies. *Environ. Sci. Technol.* **2000**, *34*, 3495−3500.
(37) Li, T.; Farrell, J. Electrochemical investigation of the rate-limiting mechanisms for trichloroethylene and carbon tetrachloride reduction at iron surfaces. *Environ. Sci. Technol.* **2001**, *35*, 3560−3565.
(38) Oh, S.-Y.; Cha, D. K.; Chiu, P. C. Graphite-mediated reduction of 2,4-dinitrotoluene with elemental iron. *Environ. Sci. Technol.* **2002**, *36*, 2178−2184.
(39) Wang, J.; Farrell, J. Investigating the role of atomic hydrogen on chloroethene reactions with iron using Tafel analysis and electrochemical impedance spectroscopy. *Environ. Sci. Technol.* **2003**, *37*, 3891−3896.
(40) Scherer, M. M.; Balko, B. A.; Tratnyek, P. G. The Role of Oxides in Reduction Reactions at the Metal−Water Interface. In *Mineral−Water Interfacial Reactions: Kinetics and Mechanisms*; Sparks, D. L., Grundl, T. J., Eds.; American Chemical Society: Washington, DC, 1998; pp 301−322.
(41) Pecher, K.; Haderlein, S. B.; Schwarzenbach, R. P. Reduction of polyhalogenated methanes by surface-bound Fe(II) in aqueous suspensions of iron oxides. *Environ. Sci. Technol.* **2002**, *36*, 1734−1741.
(42) Deng, B.; Hu, S.; Whitworth, T. M.; Lee, R. Trichloroethylene Reduction on Zero-Valent Iron: Probing Reactive Versus NonReactive Sites. In *Chlorinated Solvent and DNAPL Remediation: Innovative Strategies for Subsurface Cleanup*; Henry, S. M., Warner, S. D., Eds.; American Chemical Society: Washington, DC, 2003; pp 181−205.
(43) White, A. F.; Peterson, M. L.; Hochella, M. F., Jr. Electrochemistry and dissolution kinetics of magnetite and ilmenite. *Geochim. Cosmochim. Acta* **1994**, *58*, 1859−1875.
(44) Odziemkowski, M. S.; Schuhmacher, T. T.; Gillham, R. W.; Reardon, E. J. Mechanism of oxide film formation on iron in simulating groundwater solutions: Raman spectroscopic studies. *Corros. Sci.* **1998**, *40*, 371−389.
(45) Lee, W.; Batchelor, B. Abiotic reductive dechlorination of chlorinated ethylenes by iron-bearing soil minerals. 1. Pyrite and magnetite. *Environ. Sci. Technol.* **2002**, *36*, 5147−5154.

Received for review March 9, 2005. Revised manuscript received August 9, 2005. Accepted August 24, 2005.

ES050472J